

BINP 99-54
hep-ph/9906387

***J/Ψ* THEORY REVIEW**
or
FROM *J* TO *Ψ*

Victor Chernyak

Budker Institute of Nuclear Physics, Novosibirsk, Russia

Talk given at the International Workshop

” e^+e^- collisions from ϕ to J/Ψ ”

1-5 March 1999, Novosibirsk

CONTENT

- 1) Hard exclusive processes in QCD: main characteristic properties
- 2) Experimental and theoretical status of J/Ψ and Ψ' decays

I. Asymptotics of exclusive amplitudes in QCD.

Exclusive processes are those in which not only the initial, but also the final state is completely specified.¹ Therefore, all experimentalists dealt with exclusive processes, but may be not all of them recognized this.

In what follows, we will be interested in two types of exclusive processes: a) reactions $e^+e^- \rightarrow \gamma^* \rightarrow H_1 H_2$, where H_1 and H_2 are two definite hadrons, mesons or baryons; these reactions determine electromagnetic form factors of hadrons, both elastic and transition ones; b) decays of the heavy quarkonium into two definite light hadrons, say $J/\Psi \rightarrow \rho\pi$, $J/\Psi \rightarrow \pi\pi$, etc.

Starting from the original papers [1, 2], the general theory of hard – i.e. those at large energies and with large momentum transfers – exclusive processes in QCD was well developed, see i.e. [3]. In particular, it has been

¹ In contrast, the inclusive process does not specifies the final state and is a sum of all possible exclusive final states. The well known example is the deep inelastic scattering $e+p \rightarrow e'+X$, for which the cross section includes summation over all possible final states X .

shown that, due to the asymptotic freedom of QCD, the leading power behaviour is determined by the connected Born diagrams, while loop corrections result only in an additional slow logarithmic evolution, similarly to the deep inelastic scattering.

For instance, the leading power behaviour of the electromagnetic form factor at $Q^2 \rightarrow \infty$ can be obtained as follows. In the Breit frame, the initial and final hadrons move along the z-axis with large momenta, $p_{1z} = (Q/2)$, $p_{2z} = (-Q/2)$. So, the quarks inside hadrons also have large longitudinal momenta: $k_z^i = x_i p_{1z}$ and $q_z^i = y_i p_{2z}$ for the initial and final quarks respectively, where x_i, y_i are the hadron momentum fractions carried by the i-th quark, $0 \leq x_i, y_i \leq 1$. At the same time, all quark transverse momenta remain small, $k_{x,y}^i \sim q_{x,y}^i \sim \Lambda_{QCD}$. Thus, to obtain the leading contribution to the matrix element of the electromagnetic current $\langle H_2(p_2) | J_\mu | H_1(p_1) \rangle$, it is legitimate to neglect the quark transverse momenta at all, as well as their binding energy inside hadrons which is also $\sim \Lambda_{QCD}$, and to replace the initial and final hadron states by a set of free collinear quarks, see figs.1,2. ² One obtains then for the meson, see fig.1 : $\langle M(p_2) | J_\mu | M(p_1) \rangle \sim \langle \bar{d}(y_2 p_2), u(y_1 p_2) | J_\mu | \bar{d}(x_2 p_1), u(x_1 p_1) \rangle \sim (\sqrt{E_2})^2 (1/Q) (1/Q^2) (\sqrt{E_1})^2 \sim (1/Q)$. The above factors originate from: a) two final quark spinors, each behaving as $\sim \sqrt{E_2} \sim \sqrt{Q}$; b) the quark propagator $\sim (1/Q)$; c) the gluon propagator $\sim (1/Q^2)$; d) two initial quark spinors, each behaving as $\sim \sqrt{E_1} \sim \sqrt{Q}$. For the pion, for instance, because $\langle \pi^+(p_2) | J_\mu | \pi^+(p_1) \rangle = (p_1 + p_2)_\mu F_\pi(Q^2)$ and $p_1 \sim p_2 \sim Q$, it follows from the above expression that the pion form factor behaves as: $F_\pi(Q^2) \sim (1/Q^2)$. In the same way, one obtains for the nucleon matrix element, fig.2: $\langle N(p_2) | J_\mu | N(p_1) \rangle \sim (\sqrt{E_2})^3 (1/Q)^2 (1/Q^2)^2 (\sqrt{E_1})^3 \sim (1/Q^3)$. Because $\langle N(p_2) | J_\mu | N(p_1) \rangle \sim \bar{N}_2 \gamma_\mu N_1 \cdot F_N(Q^2)$, where N_1 and \bar{N}_2 are the initial and final nucleon spinors (each behaving as $\sim \sqrt{Q}$) and $F_N(Q^2)$ is the nucleon form factor, it follows from the above that $F_N(Q^2) \sim 1/Q^4$.

In fact, proceeding in the above described simplest way one obtains the highest possible power behaviour of form factors and, similarly, of any other hard exclusive amplitude. The real behaviour of amplitudes can be additionally power suppressed depending on the quantum numbers of the initial and final hadrons. There are two main selection rules for these additional suppressions [1].

a). The first one is relevant for the higher helicity hadron states: $|\lambda| = |S_z| > 1$ for mesons and $|\lambda| > 3/2$ for baryons. Such meson helicities can not be made from the quark spin projections, $S_{z1}, S_{z2} = (\pm 1/2)$, which means the quarks have necessarily a nonzero angular momentum projection $L_z = [\lambda - S_{z1} - S_{z2}] \neq 0$ in such a state ³, and its wave function Φ_i contains the factor $\sim \exp\{iL_z\phi\}$.

The total transition amplitude is a product of the initial and final hadron

² On figures: the thick line is the charm quark, the thin line is the light quark, the dashed line is the gluon, the wavy line is the photon.

³ Considering here the valence wave function component, i.e. those with the minimal number of constituents.

wave functions, Φ_i and Φ_f^* , with the hard kernel T (which is a product of all intermediate quark and gluon propagators), integrated over the quark relative momenta inside the initial and final hadrons. These integrations include in particular $\int_0^{2\pi} d\phi$ (and similarly for other hadrons). So, with respect to the angle ϕ , the transition amplitude contains the factor:

$$\int_0^{2\pi} d\phi \exp\{iL_z\phi\} T(Q, x_j, \mathbf{k}_\perp, \dots) .$$

The ϕ -dependence appears in T through its dependence on the quark transverse momenta in the state Φ_i : $k_\perp^\pm = (k_x \pm ik_y) = |\mathbf{k}_\perp| \exp\{\pm i\phi\}$. The hard kernel can be thought as being decomposed into a series in powers of k_\perp^+ and k_\perp^- . Then, the above integration separates out the term $\sim \exp\{-iL_z\phi\}$ from this series, while all terms $\sim \exp\{-iL'_z\phi\}$ with $L'_z \neq L_z$ will give zero after integration over ϕ .

The crucial point is that "the hard kernel is hard", i.e. intermediate quark and gluon propagators have virtualities $\sim Q^2$, due to large longitudinal momentum transfers $\sim Q$. On the other hand, the typical quark transverse momenta inside the hadron are small, $|\mathbf{k}_\perp| \sim \Lambda_{QCD}$. So, the quark transverse momenta give only small power corrections in the hard kernel. The expansion of the hard kernel looks schematically as follows: $T = Q^{-n} [1 + (k_\perp^\pm/Q) + (k_\perp^\pm/Q)^2 + \dots]$. Therefore, the needed term extracted from the hard kernel will have the additional suppression $\sim (k_\perp^-/Q)^{L_z} \sim (\Lambda_{QCD}/Q)^{L_z} \exp\{-iL_z\phi\}$, in comparison with the leading behaviour of the hard kernel.⁴

Thus, the final result is that for those hadron states which require the wave function components with $L_z \neq 0$, each unit of $|L_z|$ will result in the additional suppression factor $\sim (1/Q)$ in the amplitude. Therefore, *the leading contribution to the hard exclusive amplitudes originates only from the hadron wave functions components with $L_z = 0$, in which the hadron helicity is a sum of spin projections of its constituent quarks: $\lambda = \mathbf{n} \cdot \mathbf{J} = \sum_i (\mathbf{n} \cdot \mathbf{S}_i)$* . Let us emphasize that *it is $L_z \neq 0$, not the angular momentum $L \neq 0$ by itself*, which leads to the amplitude suppression. So, *the hard exclusive amplitudes for those mesons and baryons which are the P , D , etc. – states in the quark model are not power suppressed in comparison with the S -state hadrons*. The reason is that the light quarks are relativistic inside the hadrons and, besides, Q is much larger than hadron masses, while the power suppression of amplitudes for the $L \neq 0$ states is right in the completely nonrelativistic situation only.

b) The second selection rule is much more evident. It can be formulated as follows: *the quark helicities are conserved inside the hard kernel*. This originates from the fact that in QCD (like QED) the helicity of the energetic quark is conserved in perturbation theory, because the quark-gluon interaction is vectorlike. For this reason, the perturbative helicity flip amplitude is $\sim (m_q/E)$, in comparison with the helicity conserving one. Because the current (i.e. entering the QCD Lagrangean) masses of the u -, d - and s -

⁴This is for $L_z > 0$; for $L_z < 0$ the corresponding term is $\sim (k_\perp^+/Q)^{(-L_z)}$.

quarks are small, $m_u \simeq 4 \text{ MeV}$, $m_d \simeq 7 \text{ MeV}$, $m_s \simeq 150 \text{ MeV}$, the corrections to the leading term from such helicity flip contributions are small for the strange quark, $\sim (m_s/Q)$, and tiny for the $u-$ and $d-$ quarks.

It seems at first sight that much larger helicity flip contributions can originate from the dynamically generated (as a result of nonperturbative interactions leading to spontaneous breaking of the axial symmetry) constituent quark masses, which are at low quark virtualities: $M_{u,d}^{\text{const}} \simeq 350 \text{ MeV}$, $M_s = m_s + M_s^{\text{const}} \simeq 500 \text{ MeV}$. Really, this is not the case. The reason is that the constituent quark masses M_i^{const} are "soft", unlike the current quark masses m_i which are "hard". This means that the current quark mass is only weakly (logarithmically) dependent on the quark virtuality, while the constituent quark mass, generated by soft nonperturbative interactions, tends quickly to zero at high virtualities: $M_i^{\text{const}}(k^2) \sim \langle 0|\bar{\psi}\psi|0\rangle/k^2 \sim \Lambda_{QCD}^3/k^2$. So, $M_i^{\text{const}}(k^2)$ give really only small power corrections inside the hard kernel, because the quark virtualities are large here: $k_i^2 \sim Q^2$. The same considerations are applicable to all other nonperturbative effects, not only to those connected with generation of M^{const} . Because all nonperturbative interactions are "soft", i.e. their effects are power suppressed at high virtualities $\sim (\Lambda_{QCD}^2/k^2)^n$, they all produce only power corrections inside the hard kernel.

The quark helicity shows its spin projection onto its momentum. But the directions of the quark and the hadron momenta do not coincide exactly because quarks inside hadrons have nonzero transverse momenta, k_\perp^i . Let us recall once more, however, that the quark longitudinal (i.e. along the hadron momentum) momentum is proportional to the hadron momentum, $k_\parallel^i = x_i|\mathbf{p}| \sim Q$, while their transverse momenta remain small, $k_\perp^i \sim \Lambda_{QCD}$. So, the angle between the quark momentum and the hadron momentum is small, $\theta \sim (|k_\perp|/k_\parallel) \sim (\Lambda_{QCD}/Q)$. Thus, up to these power corrections, the conservation of the quark helicity is equivalent to conservation of its spin projection onto the momentum of the hadron it belongs.

Taken alone, this does not lead to immediate consequences for hadron helicities because the hadron helicity differs in general from the sum of quark spin projections when $L_z \neq 0$. But being combined with the point "a" above that $L_z = 0$ for the leading contributions, the net result is *a conservation of hadron helicities in the leading contributions to all hard exclusive amplitudes*. These include in particular all diagonal and transition form factors, the heavy quarkonium decays into light hadrons, etc.

All the above considerations and selection rules are summarized by a simple formula for the asymptotic power behaviour of any form factor [1]:

$$\langle p_2, J_2, \lambda_2 | J_\lambda | p_1, J_1, \lambda_1 \rangle \sim \left(\frac{1}{Q} \right)^{(n_1^{\min} + n_2^{\min} - 3) + |\lambda_2 - \lambda_1|}. \quad (1)$$

Here: p_i , J_i , λ_i are the initial and final hadron momenta, spins and helicities respectively; λ is the photon helicity and $\lambda = (\lambda_1 + \lambda_2)$ in the Breit

frame; n_i^{min} are the minimal possible numbers of constituents inside the given hadron: $n^{min} = 2$ for mesons and $n^{min} = 3$ for baryons. The hadron helicity conservation is clearly seen from eq.(1). Moreover, it determines the behaviour of all nonleading form factors.

In agreement with the explanations given above, *the asymptotic behaviour is independent of hadron spins, parities etc., and only helicities are the relevant quantum numbers*. Besides, increasing the number of constituents results in additional suppression, so that the nonvalence components (i.e. those containing additional gluons or quark-antiquark pairs) of the hadron wave functions give power suppressed corrections.⁵

II. J/Ψ and Ψ' decays

As was described above, there are simple rules allowing one to obtain the leading power term of any exclusive amplitude at $Q \rightarrow \infty$, and a large number of concrete calculations has been performed, see i.e. [3]. As for the loop corrections to the Born contributions, they are amenable to standard perturbation theory calculations and result in a slow additional logarithmic evolution with increasing Q , see [1-3].

Up to now, however, there remains the main unsolved problem in all practical applications – to calculate (or to estimate reliably, at least) the power corrections to the leading terms. These power corrections, which are negligible in the formal limit $Q \rightarrow \infty$, may be of real importance when comparing the leading term calculations with the present data which have typically $Q = 2 - 4 \text{ GeV}$. It seems at first sight that $Q \simeq 3 \text{ GeV}$, which corresponds to charmonium decays, is sufficiently large in comparison with the scale of power corrections which is typically $\simeq \Lambda_{QCD} \simeq 350 \text{ MeV}$. The matter is, however, that the role of power corrections is determined actually not by the ratio (Λ_{QCD}/Q) , but rather by (Λ_{QCD}/Q_{eff}) , with $Q_{eff} \ll Q$. To illustrate, let us consider the $J/\Psi \rightarrow K^* K$ decay. In the J/Ψ rest frame the momentum of each light meson is $|\mathbf{p}| = 1.37 \text{ GeV}$. It is shared however between two its constituent quarks, so that the longitudinal momentum of each quark is roughly: $k_{\parallel} \simeq |\mathbf{p}|/2 \simeq 680 \text{ MeV}$, which is only a factor two larger than its transverse momentum $|\mathbf{k}_{\perp}| \simeq 350 \text{ MeV}$. So, the power corrections to the leading term due to $|\mathbf{k}_{\perp}| \neq 0$ can be $\simeq 50\%$ in the amplitude.

The size of power corrections can be estimated also in a pure kinematical way. Say, the $J/\Psi \rightarrow b_1(1235)\pi$ decay amplitude contains the term $\sim (e_{\mu}^{\lambda_0} \epsilon_{\mu}^{\lambda_1})$, where e^{λ_0} and ϵ^{λ_1} are the polarization vectors of J/Ψ and b_1 respectively. At large values of the b_1 -momentum: $\epsilon_{\mu}^{\lambda_1=0} = (p_{\mu}/M_{b_1}) + O(M_{b_1}/|\mathbf{p}|)$, while $\epsilon_{\mu}^{|\lambda_1|=1} = O(1)$. So, the production of the $|b_1^{|\lambda_1|=1}\pi\rangle$ -state will be power

⁵ In fact, the above given explanations were somewhat simplified. For instance, the wave function of the meson state with $\lambda = 2$ contains not only the two quark component with $S_{z1} = S_{z2} = 1/2$, $L_z = 1$, but also, say, the nonvalence component with the additional gluon, such that: $S_{z1} = S_{z2} = 1/2$, $S_{z3} = 1$, $L_{zi} = 0$. It is not difficult to see that the final result remains the same. The form factor gains $\sim Q$ due to $L_z = 0$ here instead of $L_z = 1$ in the two quark component, but losses $\sim 1/Q$ because $n_1 = 3$ now.

suppressed, $\sim (M_{b_1}/|\mathbf{p}|)$, in comparison with those of $|b_1^{\lambda_1=0}\pi\rangle$. Really however the suppression is absent as $(M_{b_1}/|\mathbf{p}|) = 0.95$ in the $J/\Psi \rightarrow b_1\pi$ decay. On the other hand, such kinematical power corrections can be taken under control, unlike the "dynamical" power corrections mentioned in the preceding paragraph.

On the whole, the heavier are final mesons the worse is a situation, and it is even worse for two baryon decays as the baryon momentum is shared between its three quarks.

These simple estimates show that there are no serious reasons to expect that formally leading terms will really dominate the charmonium decay amplitudes.

In particular, there are no reasons to expect that the above described helicity selection rules will be actually operative here, as the factor $\simeq (1/2)$ "suppression" (see above) can be easily overwhelmed by others numerical factors. For instance, the formally leading contribution to $J/\Psi \rightarrow VT$ and $J/\Psi \rightarrow AP$ decays gives the fig.3 diagram ⁶ in which the meson wave functions contain the minimal number of constituents, and with no helicity flips. Due to a loop however, it contains the additional smallness $\simeq (\bar{\alpha}_s/\pi) \simeq 0.1$, so that the figs.4-6 diagrams which are formally suppressed $\sim (\Lambda_{QCD}/Q_{eff})$ due to the nonvalence (i.e. three particle) wave functions, give really larger contributions.

Thus, it looks somewhat strange that a number of authors insist that those amplitudes which are helicity suppressed (or contain the nonvalence wave function components which give the same effect) in the formal limit $Q \rightarrow \infty$, will be actually heavily suppressed in charmonium decays. The experiment shows that this is not the case. For instance, the $(J/\Psi \rightarrow \omega\pi)$ -decay amplitude is formally helicity suppressed while $(J/\Psi \rightarrow \pi^+\pi^-)$ is not, but [4] : $\text{Br}(J/\Psi \rightarrow \omega\pi)/\text{Br}(J/\Psi \rightarrow \pi^+\pi^-) \simeq 3$.

A large number of various Ψ' decays has been measured by the BES Collaboration during last time [5-7], and these very interesting results were presented at this workshop by Prof. Stephen L. Olsen [8]. So, it is a great challenge for theory to understand and explain these data.

When comparing the J/Ψ and Ψ' decays into light hadrons, it will be wrong to compare the branchings by itself. The reason is that Ψ' , unlike J/Ψ , decays mainly to lower charmonium states. Besides, the values of the Ψ' and J/Ψ wave functions at the origin are different. To avoid both these differences, one rather has to compare the ratios: $\text{Br}(\Psi' \rightarrow X)/\text{Br}(\Psi' \rightarrow e^+e^-)$ and $\text{Br}(J/\Psi \rightarrow X)/\text{Br}(J/\Psi \rightarrow e^+e^-)$. In other words, one has to rescale the Ψ' -branchings by the factor [4]: $\text{Br}(\Psi' \rightarrow e^+e^-)/\text{Br}(J/\Psi \rightarrow e^+e^-) = 0.14$. Actually, this is not the only scale factor, as the mass of Ψ' is noticeably higher than those of J/Ψ : $(M_{\Psi'}^2/M_{\Psi}^2) = 1.4$, and the exclusive branchings have a high power dependence on the initial mass, $\sim (1/M)^{n_{eff}}$,

⁶ Ψ_i means J/Ψ or Ψ' , in this diagram and in all others.

see tables. So, it seems reasonable to separate out this dependence which is, besides, quite different for different decay channels. On the whole, we have to compare the "reduced" decay amplitudes, A and A' for J/Ψ and Ψ' respectively, from which both the above described rescaling factors are separated out. In the tables 1-5 given below I have tried to recalculate these reduced amplitudes from the experimental data (taking into account also the phase space corrections).

Now, the natural expectation is that, in a "normal situation", these reduced amplitudes A' and A will be close to each other, so that $R = |A'/A|$ will be close to unity. As it is seen from the tables 1-5, the situation is not "normal". Some decay channels are strongly suppressed ($R \ll 1$), while other ones are significantly enhanced ($R > 1$).

The most famous is the " $\rho\pi$ -puzzle", i.e. a very small value of $\text{Br}(\Psi' \rightarrow \rho\pi)/\text{Br}(J/\Psi \rightarrow \rho\pi)$, see table 1. A number of speculative explanations have been proposed, including even so exotic as a significant admixture of the charm component, $(\bar{C}C)$, in the ρ -meson wave function [9]. Most of speculations are based on the idea that $\Psi' \rightarrow \rho\pi$ is "naturally small" because the decay amplitude is helicity suppressed, while $J/\Psi \rightarrow \rho\pi$ is "abnormally large". So, the efforts were concentrated on searching the sources of this enhancement: especially introduced nearby gluonium resonance [10], or a large admixture of the colored component in the J/Ψ -wave function, unlike the Ψ' one [11], etc.

As was pointed out above, the helicity suppression is not really a strong effect in the charmonium region as its typical value is only $\simeq 1/2$ here, and it is easily overwhelmed by other numerical factors. So, the whole above idea does not look very appealing. Moreover, the (hopefully) main contributions to $J/\Psi \rightarrow \rho\pi$ have been directly calculated long ago in [12] (see also [3], ch. 9.1). These originate from the figs.4-5 diagrams and give: $\text{Br}(J/\Psi \rightarrow \rho\pi) \simeq 1\%$. This shows clearly that the experimental value: $\text{Br}(J/\Psi \rightarrow \rho\pi) = (1.27 \pm 0.09)\%$ [4] is natural and there is no need for an additional enhancement.

So, we come naturally to the idea that it is not $J/\Psi \rightarrow \rho\pi$ which is enhanced, but rather $\Psi' \rightarrow \rho\pi$ which is suppressed. What may be the reason? Looking at tables 1-5 one sees that the underlying mechanism is highly nontrivial and is of dynamical nature as it operates selectively, suppressing some channels and enhancing other ones. The possible explanation has been proposed long ago in [3] (ch. 8.4). The idea is that Ψ' , unlike J/Ψ , is really a highly excited state, – it is close even to the $\bar{D}D$ -threshold! So, it looks natural that there is a large admixture of the nonvalence – i.e. those containing the additional gluon or the light quark-antiquark pair – components in its wave function. If so, its decays into various channels can differ significantly from those of J/Ψ , for which the nonvalence component is expected to be less significant because it is the lowest state. Unfortunately, this idea also remains a pure speculation, as no concrete calculations were performed up to now. So, by necessity, our discussion below will be more

qualitative than quantitative.

2.1 VP - decays (see table 1). As for the strong amplitudes, the main diagrams are expected to be those shown on figs.4-6. For Ψ' , according to the above described idea, the diagrams like those shown on fig.7 (and many others similar) are expected to be also of importance. Let us emphasize that, even in the formal limit $Q = M_{\Psi'} \rightarrow \infty$, these nonvalence contributions are not power suppressed here in comparison with the valence ones. Indeed, two out of three gluon propagators in the diagram on fig.7 (denoted by open circles) are semihard, i.e. their virtuality is parametrically only $k_i^2 \sim p_o Q$, rather than $\sim Q^2$, where p_o is the light quark bound state momentum in the Ψ' -rest frame. This gains the factor $\sim (Q^2/p_o^2)$. Besides, the ω and pion wave functions are two-particle here and both can have the leading twist. This gains the factor $\sim (Q/\Lambda_{QCD})$, in comparison with the figs.4-6 contributions where one out of two mesons has the nonleading twist three-particle wave function. The whole gained factor $\sim (Q^3/p_o^2 \Lambda_{QCD})$ compensates for the additional smallness $\sim (p_o^3/Q^3)$ due to the additional $(\bar{q}q)$ -pair in the 4-particle component of the Ψ' -wave function.

So, the proposed here explanation of the $\rho - \pi$ -puzzle is that the valence and nonvalence strong contributions interfere destructively in this channel and, as a matter of case, cancel to a large extent in the total $\Psi' \rightarrow \rho\pi$ strong amplitude, while the role of nonvalence contributions is much less significant in $J/\Psi \rightarrow \rho\pi$. From this viewpoint, there is no deep reason for the experimentally observed very strong suppression of $\Psi' \rightarrow \rho\pi$, this is a result of a casual cancelation.

2.2 VT and AP - decays (see table 2). These decays are the leading ones in the formal limit $Q \rightarrow \infty$. However, these formally leading contributions originate from the loop diagram, fig.3, and thus contain the additional loop smallness $\simeq (\bar{\alpha}_s/\pi) \simeq 0.1$. Therefore, they are small really in comparison with contributions of the figs.4-6 diagrams which are expected to be dominant in the J/Ψ -decays. Thus, the prediction is that all $J/\Psi \rightarrow (VP, VT, AP)$ decays receive main contributions from the figs.4-6 diagrams and will be of comparable strength, and this is the case, see tables 1-2. As for the $\Psi' \rightarrow (VT, AP)$ decays, it is seen from the table 2 that the sign of the interference of valence and nonvalence contributions is opposite in these two channels, so that the VT - decays are suppressed while the AP - ones are enhanced.

2.3 $\bar{B}B$ - decays (see table 3). It is seen from the table 3 that all baryon decays are enhanced at Ψ' . This may result from the nonvalence contributions like those shown in fig.8 (and others similar), interfering constructively with the valence contributions from the diagram on fig.9.

2.4 PP and VV - decays (see table 4). There is a number of "puzzles". First, the $\pi^+\pi^-$ -mode which is electromagnetic is (it seems, the error bars are large) strongly enhanced at Ψ' , in comparison with that at J/Ψ . If this decay mode were solely due to the pion form factor $F_\pi(Q^2)$, fig.10, this will imply $F_\pi(M_{\Psi'}^2) \simeq 2 F_\pi(M_{J/\Psi}^2)$. But this is impossible because $F_\pi(Q^2)$

decreases with Q^2 , like $\sim 1/Q^2$. So, this is a strong indication that the nonvalence contributions (like those shown on fig.11, and many others similar) are of great importance here. This is not the whole story however, as $\text{Br}(J/\Psi \rightarrow \pi^+ \pi^-)$ is too large by itself. If it were solely due to $F_\pi(Q^2)$, then it will result in: $F_\pi(M_{J/\Psi}^2) \simeq 1 \text{ GeV}^2/M_{J/\Psi}^2$, while most of theoretical estimates do not exceed $\simeq (0.5 - 0.6) \text{ GeV}^2/M_{J/\Psi}^2$. So, we come to a conclusion that, in this channel, the nonvalence contributions are of importance even for J/Ψ .

If really important, the nonvalence contributions like those shown on the fig.11 diagram will have also another impact. The matter is that their SU(3) flavour structure is different from those of the fig.10 diagram, and this possibility was ignored in all phenomenological descriptions of $J/\Psi \rightarrow PP$ - decays (and similarly for the nonvalence electromagnetic contributions in other decay channels). So, such contributions can influence, in particular, the conclusions about $\sim 90^\circ$ relative phases of the strong and electromagnetic contributions to the decay amplitudes.

2.5 ($J/\Psi, \Psi' \rightarrow \omega \pi^0$) - decays (see table 1). This channel is electromagnetic (i.e. it needs photon) and is very interesting. Suppose first that it is solely due to the $\gamma \omega \pi$ - form factor $F_{\omega \pi}(Q^2)$, fig.10. This last is helicity suppressed and has the asymptotic behaviour: $\sim (1/Q^4)$.⁷ The data at $Q^2 \leq 5 \text{ GeV}^2$ are sufficiently well described by a sum of $\rho(770)$ and $\rho'(1460)$ contributions. Being not too close to these resonances, we can neglect the widths, and it will be given then by a simple expression:

$$F_{\omega \pi}(Q^2) = F_{\omega \pi}(0) \frac{m_\rho^2 M_{\rho'}^2}{(m_\rho^2 - Q^2)(M_{\rho'}^2 - Q^2)} ; \quad F_{\omega \pi}(0) = 2.3 \text{ GeV}^{-1}. \quad (2)$$

But the eq.(2) fails to describe the $J/\Psi \rightarrow \omega \pi$ and $\Psi' \rightarrow \omega \pi$ decays, as this will require much larger value of $F_{\omega \pi}(Q^2 = M_{J/\Psi}^2)$ and especially of $F_{\omega \pi}(Q^2 = M_{\Psi'}^2)$. Moreover, the reaction $e^+ e^- \rightarrow \omega \pi^0$, which by definition determines $F_{\omega \pi}(Q^2)$, has been measured recently by the BES Collaboration. The results [8] for $F_{\omega \pi}(Q^2)$ are presented on fig.12, together with previous data at smaller Q^2 [13, 14]. The curve is from eq.(2). It is seen that the new data agree with eq.(2), while both J/Ψ and Ψ' lie well above. This shows unambiguously that both $(J/\Psi \rightarrow \omega \pi)$ and $(\Psi' \rightarrow \omega \pi)$ - decay amplitudes contain, besides $F_{\omega \pi}$, additional significant contributions, and these last are larger for Ψ' than for J/Ψ . All this agrees with the additional nonvalence contributions, like those shown on the fig.13 diagram (and many others similar; here too these nonvalence contributions are not power suppressed in comparison with the valence ones, even in the formal limit $Q \rightarrow \infty$).

2.6 ($J/\Psi, \Psi' \rightarrow \gamma \pi^0$) - decays (see table 5). There are two main contributions to the $(J/\Psi \rightarrow \gamma \pi^0)$ - amplitude: the VDM one, fig.14, and

⁷ $F_{\omega \pi}(Q^2)$ is defined by: $\langle \omega_\lambda(p_1) \pi^0(p_2) | J_\mu | 0 \rangle = \epsilon_{\mu\nu\sigma\tau} p_1^\nu p_2^\sigma e_\lambda^\tau \cdot F_{\omega \pi}(Q^2)$. The helicity of ω is $|\lambda| = 1$ here. From eq.(1), this matrix element behaves as $\sim (1/Q^2)$, resulting in $F_{\omega \pi}(Q^2) \sim (1/Q^4)$, because $p_1 \sim p_2 \sim Q$, $e_\lambda \sim 1$.

through the intermediate photon, fig.15. They were calculated in [12] (see also [3], ch.5.4) with the result: $\text{Br}(J/\Psi \rightarrow \gamma\pi^0) \simeq 4 \cdot 10^{-5}$, in agreement with data. The relative contributions to the decay amplitude from these diagrams are here: (fig.14):(fig.15) $\simeq (1.6 : 1.0)$. When going from J/Ψ to Ψ' , the radical difference emerges from the strong suppression of the VDM contribution for Ψ' due to nonvalence contributions, while these last do not influence the amplitude with the intermediate photon. Thus, the relative contributions to the decay amplitude become now (using the BES data for $\Psi' \rightarrow \rho\pi$, see table 1): (fig.14):(fig.15) $\simeq (0.3 : 1.0)$, and $\text{Br}(\Psi' \rightarrow \gamma\pi^0)$ will be $\simeq 1 \cdot 10^{-6}$.

Conclusions

A large number of various exclusive Ψ' -decays has been measured by the BES Collaboration during last time. These results are very interesting not only for understanding the properties of Ψ' by itself. Comparison of Ψ' and J/Ψ decays helps to elucidate the properties of both of them, as well as properties of strong interaction at these energies.

In particular, these measurements revealed that, fortunately or unfortunately, the situation is much more complicated than the naive expectations based on the dominance of formally leading (at $Q \rightarrow \infty$) terms. This especially concerns Ψ' which is a highly excited state close to the $\bar{D}D$ -threshold.

The present status of theory is such that, it seems, there is some understanding of the J/Ψ and Ψ' - decays on the qualitative and sometimes on the semiquantitative level, but a lot of job remains to be done to have a really quantitative description of these decays.

As it is clear from the above considerations, it will be of great interest and of great help for theory if our colleagues experimentalists will be able to measure some distinguished electromagnetic processes somewhere in the region $8 \text{ GeV}^2 < Q^2 < 16 \text{ GeV}^2$, but out of J/Ψ and Ψ' (like the recent measurement of $e^+e^- \rightarrow \omega\pi$ by the BES Collaboration, see fig.12). They are: $e^+e^- \rightarrow \{\pi^+\pi^-, K^+K^-, \rho\eta, \rho\eta', \gamma\pi, \gamma\eta, \gamma\eta'\}$. These measurements will determine the corresponding form factors which are of great interest by itself and will be useful for elucidating the electromagnetic contributions into the J/Ψ and Ψ' - decays. Besides, it will be very useful to improve the poor accuracy of $\Psi' \rightarrow \pi^+\pi^-$ and $\Psi' \rightarrow K^+K^-$ and to measure $\Psi' \rightarrow \bar{K}^0K^0$.

Acknowledgments

I am deeply grateful to L.M. Barkov, A.E. Bondar, B.I. Khazin and S.I. Serednyakov for useful discussions and critical remarks, and to N.I. Root for preparing the figure 12.

This work is supported in part by the grant INTAS 96-155.

References

- [1] V.L. Chernyak and A.R. Zhitnitsky, JETP Lett., **25** (1977) 510;
Sov J. Nucl. Phys., **31** (1980) 544.
- [2] V.L. Chernyak, V.G. Serbo and A.R. Zhitnitsky, JETP Lett.,
26 (1977) 594; Sov. J. Nucl. Phys., **31** (1980) 552.
- [3] V.L. Chernyak and A.R. Zhitnitsky, Phys. Rep. **112** (1984) 173.
- [4] Particle Data Group, Europ. Phys. J., **C 3** (1998) 1.
- [5] BES Collaboration, Phys.Rev., **D 58** (1998) 097101.
- [6] BES Collaboration, Phys.Rev.Lett., **81** (1998) 5080.
- [7] BES Collaboration, hep-ex/9901022.
- [8] S.L. Olsen (BES Collaboration),
Puzzles in hadronic physics around 3 GeV, These Proceedings.
- [9] S.J. Brodsky and M. Karliner, Phys.Rev.Lett., **78** (1997) 4682.
- [10] W.S. Hou and A.Soni, Pys.Rev.Lett., **50** (1983) 569;
S.J.Brodsky, G.P.Lepage and S.F.Tuan, Phys.Rev.Lett., **59**(1987)621.
- [11] Yu-Qi Chen and E. Braaten, Phys.Rev.Lett., **80** (1998) 5060.
- [12] A.R. Zhitnitsky, I.R. Zhitnitsky and V.L. Chernyak,
Yad. Fiz., **41** (1985) 199; and ref. [3], ch. 9.1, ch. 5.4.
- [13] R.R. Akhmetshin et al., CMD-2 Collaboration
Preprint BINP 98-63, Novosibirsk 1998, hep-ex/9904024.
- [14] D. Bisello et al., DM2-Collaboration,
Nucl. Phys. (Proc. Suppl.) **B 21** (1991) 11.

Table 1: $(J/\Psi, \Psi') \rightarrow VP$; $n_{eff} = 6, k = 3$

CHANNEL	$Br(\psi' \rightarrow VP) \cdot 10^4$	$Br(\psi \rightarrow VP) \cdot 10^3$	$\Delta\%$	$R = A'/A $
$\rho\pi$	< 0.83 PDG	12.7 ± 0.9	5.0	< 0.36 PDG
	< 0.28 BES	PDG		< 0.21 BES
K^+K^{*-} +c.c.	< 0.54 PDG	5.0 ± 0.4	5.0	< 0.46 PDG
	< 0.30 BES	PDG		< 0.35 BES
$\bar{K}^0 K^{*0}$ +c.c.	$0.81 \pm 0.24 \pm 0.16$ BES	4.2 ± 0.4 PDG	5.0	0.62 ± 0.14 BES
$\omega\eta$	< 0.26 BES	1.58 ± 0.16 PDG	5.0	< 0.58 BES
$\omega\eta'$	$0.76 \pm 0.36 \pm 0.15$ BES	0.17 ± 0.02 PDG	7.4	2.5 ± 0.8 BES
$\phi\eta$	$0.35 \pm 0.19 \pm 0.07$ BES	0.65 ± 0.07 PDG	5.7	1.0 ± 0.3 BES
$\phi\eta'$	< 0.75 BES	0.33 ± 0.04 PDG	6.5	< 1.9 BES
$\omega\pi^0$ (electromagnetic)	$0.38 \pm 0.17 \pm 0.11$ BES	0.42 ± 0.06 PDG	5.0	1.35 ± 0.35 BES
$\rho\eta$ (electromagnetic)	$0.21 \pm 0.11 \pm 0.05$ BES	0.19 ± 0.02 PDG	5.0	1.5 ± 0.5 BES
$\rho\eta'$ (electromagnetic)	< 0.3 BES	0.10 ± 0.02 PDG	7.4	< 2.0 BES

Here and in all other tables, the total rescaling factor Δ is:

$$\Delta = \frac{Br(\psi' \rightarrow \bar{e}e)}{Br(\psi \rightarrow \bar{e}e)} \cdot \left(\frac{M_\psi}{M_{\psi'}} \right)^{n_{eff}} \cdot \left(\frac{M_\psi \cdot p'}{M_{\psi'} \cdot p} \right)^k ,$$

where the meaning of the first factor was explained in the text, the second factor accounts for dependence of decay amplitudes on the mass of the decaying charmonium state, and the last one is the phase space correction (p and p' are the c.m.s. momenta of final particles in the $J/\Psi \rightarrow X$ and $\Psi' \rightarrow X$ decays).

The ratio of the "reduced" amplitudes is:

$$R = \left| \frac{A'}{A} \right| = \left\{ \frac{1}{\Delta} \frac{Br(\Psi' \rightarrow X)}{Br(J/\Psi \rightarrow X)} \right\}^{1/2} ,$$

where A and A' are the "reduced" amplitudes of the J/Ψ and $\Psi' \rightarrow X$ decays.

Table 2: $(J/\Psi, \Psi') \rightarrow VT, AP; n_{eff} = 6, k = 1$

CHANNEL	$\text{Br} (\psi' \rightarrow X) \cdot 10^4$	$\text{Br} (\psi \rightarrow X) \cdot 10^3$	$\Delta\%$	$R = A'/A $
$\omega f_2(1270)$	< 1.7 BES	4.3 ± 0.6 PDG	5.6	$< 0.85 \pm 0.06$ BES
$\rho a_2(1320)$	< 2.3 BES	10.9 ± 2.2 PDG	5.6	$< 0.61 \pm 0.06$ BES
$\phi f'_2(1525)$	< 0.45 BES	1.2 ± 0.2 PDG	6.6	$< 0.75 \pm 0.10$ BES
$K^{*,o} \bar{K}^o(1430)$ +c.c.	< 1.2 BES	6.7 ± 2.6 PDG	6.0	$< 0.55 \pm 0.10$ BES
$b_1^+(1235) \pi^-$	$5.3 \pm 0.8 \pm 0.8$ BES	3.0 ± 0.5 PDG	5.3	1.82 ± 0.25 BES
$K_1^+(1270) K^-$ +c.c.	$10.0 \pm 1.8 \pm 1.8$ BES	< 2.9 BES	5.4	$> 2.5 \pm 0.3$ BES
$K_1^+(1400) K^-$ +c.c.	< 2.9 BES	$3.8 \pm 0.8 \pm 0.5$ BES	5.5	$< 1.2 \pm 0.15$ BES

Table 3: $(J/\Psi, \Psi') \rightarrow \bar{B}B; n_{eff} = 8, k = 1$

CHANNEL	$\text{Br} (\psi' \rightarrow X) \cdot 10^4$	$\text{Br} (\psi \rightarrow X) \cdot 10^3$	$\Delta\%$	$R = A'/A $
$\bar{p}p$	1.9 ± 0.5 PDG	2.14 ± 0.10 PDG	3.8	1.5 ± 0.2 PDG
$\bar{\Lambda}\Lambda$	$2.11 \pm 0.23 \pm 0.26$ BES	1.27 ± 0.17 PDG	4.0	2.0 ± 0.2 BES
$\bar{\Sigma}^o \Sigma^o$	$0.94 \pm 0.30 \pm 0.38$ BES	1.8 ± 0.4 PDG	4.1	1.35 ± 0.35 BES
$\bar{\Xi}\Xi$	$0.83 \pm 0.28 \pm 0.12$ BES	1.35 ± 0.14 PDG	4.6	1.0 ± 0.2 BES
$\bar{\Delta}^{--} \Delta^{++}$	$0.89 \pm 0.10 \pm 0.24$ BES	1.10 ± 0.29 PDG	4.2	1.4 ± 0.3 BES

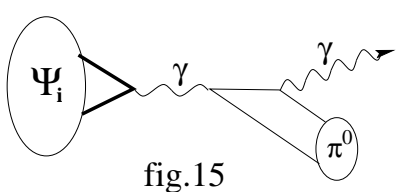
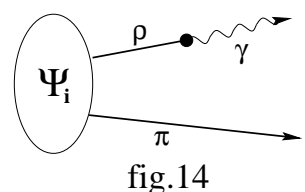
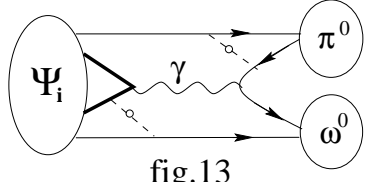
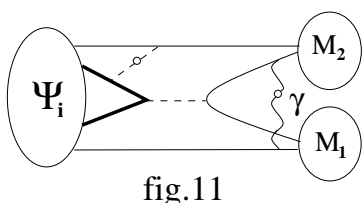
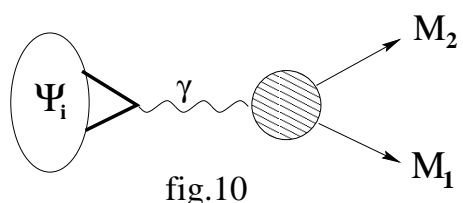
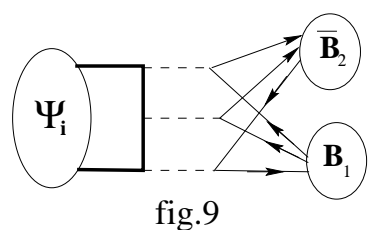
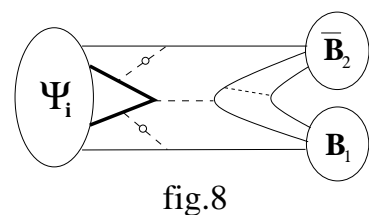
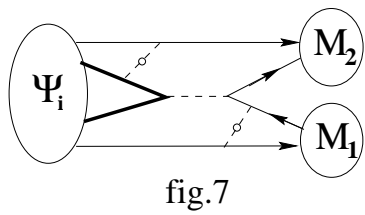
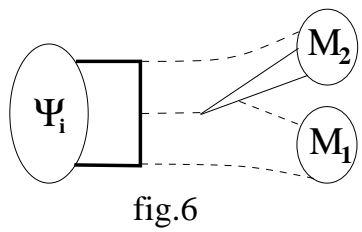
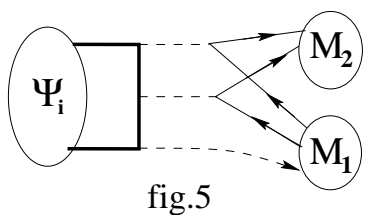
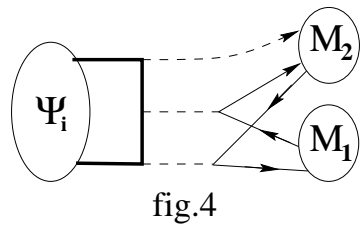
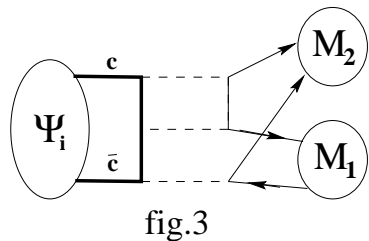
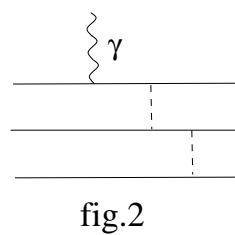
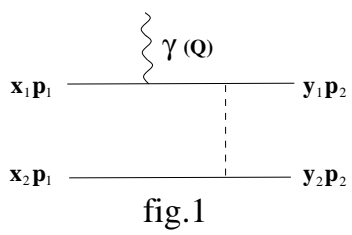
Table 4: $(J/\Psi, \Psi') \rightarrow PP, VV; n_{eff} = 4, k = 3$

CHANNEL	$\text{Br} (\psi' \rightarrow X) \cdot 10^4$	$\text{Br} (\psi \rightarrow X) \cdot 10^3$	$\Delta\%$	$R = A'/A $
$\pi^+ \pi^-$ (electromagnetic)	0.8 ± 0.5 PDG	0.15 ± 0.02 PDG	7.0	2.8 ± 0.9 PDG
$K^+ K^-$	1.0 ± 0.7 PDG	0.24 ± 0.03 PDG	7.3	2.4 ± 0.9 PDG
$\bar{K}^o K^o$		0.11 ± 0.02 PDG	7.3	
$\bar{K}^{*,o} K^{*,o}$	$0.45 \pm 0.25 \pm 0.07$ BES	< 0.5 PDG	8.6	$> 1.0 \pm 0.3$ BES

Table 5:

$$(J/\Psi, \Psi') \rightarrow \gamma P, \gamma T; n_{eff}^{(\gamma\eta, \gamma\eta')} = 4, k^{(\gamma P)} = 3; n_{eff}^{(\gamma T)} = 2, k^{(\gamma T)} = 1$$

CHANNEL	$\text{Br} (\psi' \rightarrow X) \cdot 10^4$	$\text{Br} (\psi \rightarrow X) \cdot 10^3$	$\Delta\%$	$R = A'/A $
$\gamma\eta$	$0.53 \pm 0.31 \pm 0.08$ BES	0.86 ± 0.08 PDG	7.1	0.93 ± 0.30 BES
$\gamma\eta'(958)$	$1.54 \pm 0.31 \pm 0.23$ BES	4.31 ± 0.3 PDG	7.7	0.68 ± 0.08 BES
$\gamma f_2(1270)$	$3.0 \pm 1.1 \pm 1.1$ BES	1.38 ± 0.14 PDG	10.0	1.5 ± 0.4 BES
$\gamma f'_2(1525)$		0.47 ± 0.06 PDG	11.0	
$\gamma\pi^o$	$\simeq 1 \cdot 10^{-2}$ prediction	0.039 ± 0.013 PDG		



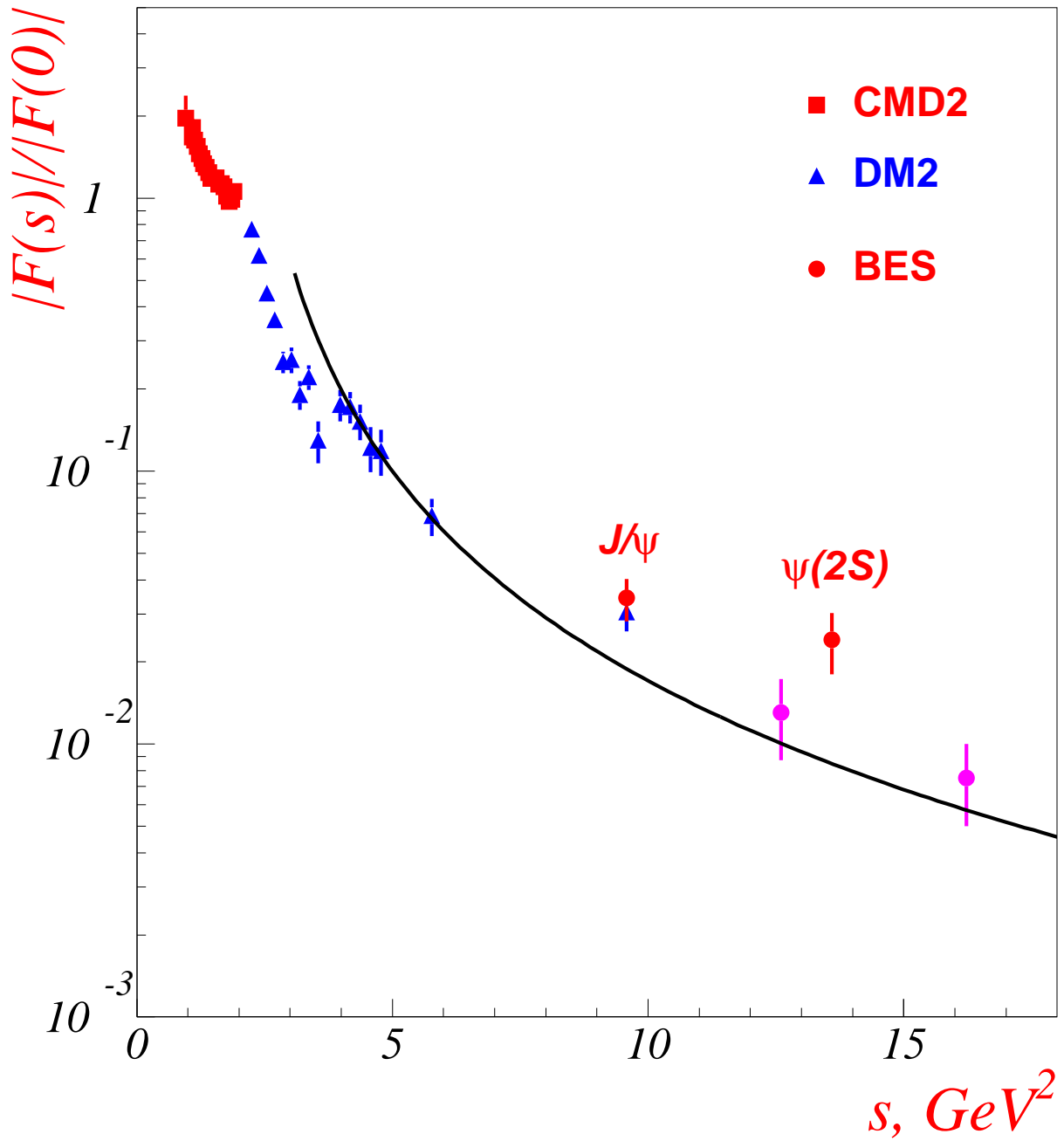


Figure 12: The curve: $\frac{F_{\omega\pi}(s)}{F_{\omega\pi}(0)} = \frac{m_\rho^2 M_{\rho'}^2}{(m_\rho^2 - s)(M_{\rho'}^2 - s)}$;
 $m_\rho = 0.77 \text{ GeV}$, $M_{\rho'} = 1.46 \text{ GeV}$